Cell, Vol. 101, 425–433, May 12, 2000, Copyright ©2000 by Cell Press

The Crystal Structure of the Ligand Binding Module of Axonin-1/TAG-1 Suggests a Zipper Mechanism for Neural Cell Adhesion

Jörg Freigang,* Karl Proba,† Lukas Leder,† Kay Diederichs,* Peter Sonderegger,† and Wolfram Welte*‡
*Faculty of Biology
University of Konstanz
Box M656
D-78457 Konstanz
Germany
†Institute of Biochemistry
University of Zurich
Winterthurerstr. 190
CH-8057 Zurich
Switzerland

Summary

We have determined the crystal structure of the ligand binding fragment of the neural cell adhesion molecule axonin-1/TAG-1 comprising the first four immunoglobulin (Ig) domains. The overall structure of axonin-$1_{Ig1–4}$ is U-shaped due to contacts between domains 1 and 4 and domains 2 and 3. In the crystals, these molecules are aligned in a string with adjacent molecules oriented in an anti-parallel fashion and their C termini perpendicular to the string. This arrangement suggests that cell adhesion by homophilic axonin-1 interaction occurs by the formation of a linear zipper-like array in which the axonin-1 molecules are alternately provided by the two apposed membranes. In accordance with this model, mutations in a loop critical for the formation of the zipper resulted in the loss of the homophilic binding capacity of axonin-1.

Introduction

Neural cell adhesion molecules (CAMs) that are expressed by neurons during neurogenesis and targeted to axons play a crucial role in axon growth and guidance along a predetermined pathway (Tessier-Lavigne and Goodman, 1996). Among these, CAMs belonging to the immunoglobulin superfamily (IgSF-CAMs) (Chothia and Jones, 1997) include transmembrane proteins, such as chicken NgCAM (Burgoon et al., 1991) and its mammalian homolog L1 (Moos et al., 1988), as well as glycosylphosphatidylinositol-anchored molecules, such as chicken axonin-1 (Zuellig et al., 1992) and its mammalian homolog TAG-1 (Furley et al., 1990). The transmembrane anchored NgCAM/L1-like glycoproteins consist in their extracellular N-terminal part of a chain of six immunoglobulin (Ig) domains followed by five fibronectin type III (FnIII) domains, whereas the glycosylphosphatidylinositol-anchored axonin-1/TAG-1-like glycoproteins are composed of six Ig domains followed by four FnIII domains (Figure 1). The IgSF-CAMs exert their function by interactions with other macromolecules, resulting in cell–cell or cell–matrix adhesion that elicits intracellular signaling (Brümmendorf and Rathjen, 1996). An IgSF-CAM may serve different cellular functions, depending on its cellular and molecular context. When displayed on the surface of axons, an IgSF-CAM may act as growth-promoting substratum, thereby promoting the orderly growth of following axons and the formation of axon bundles (Rathjen et al., 1987). When exposed on the surface of growth cones, an IgSF-CAM may serve as a sensor for a preferred substratum (Stoeckli and Landmesser, 1995). Both the substratum and the sensor function of axonal IgSF-CAMs go along with the formation of intimate membrane contacts between cell surfaces and extending growth cones (Stoeckli et al., 1996; Kunz et al., 1998).

Axonin-1/TAG-1 is one of the functionally best characterized IgSF-CAMs. It is capable of mediating cell–cell contacts by homophilic binding between molecules resident in apposed membranes (*trans* binding; Rader et al., 1993; Felsenfeld et al., 1994). Well-characterized interactions with other glycoproteins include an interaction with NgCAM bound to the same membrane (*cis*-interaction; Buchstaller et al., 1996; Stoeckli et al., 1996) and an interaction with NrCAM of another cell (*trans*-interaction; Fitzli et al., 2000). The heterophilic interaction of axonin-1 with NgCAM occurs only when both molecules are located in the same membrane, but not between molecules of different cells (Buchstaller et al., 1996). This *cis*-association of axonin-1 and NgCAM has been observed in sensory neurons cultivated at low density, i.e., without cell–cell contact (Buchstaller et al., 1996). When growing axons fasciculate due to the adhesive forces of their surface CAMs, NgCAM and axonin-1 form heterotetrameric complexes composed of one NgCAM:axonin-1 heterodimer on each membrane (Kunz et al., 1996). An interaction of growth cone axonin-1 with NrCAM displayed on the surface of floor plate cells has been identified as a crucial element in the decision taken by commissural axons of the spinal cord to grow across the midline through the floor plate (Stoeckli and Landmesser, 1995). In a recent study with explants of commissural neurons, the *trans*-interaction between axonin-1 of growth cones and NrCAM of the substratum has been demonstrated to mediate axon guidance without promoting axon elongation (Fitzli et al., 2000). In contrast, in the peripheral nervous system, growth cone axonin-1 has been found to act as an axonal receptor mediating neurite outgrowth on NrCAM (Lustig et al., 1999).

In the heterophilic interactions with NgCAM and NrCAM, the first four Ig domains of axonin-1 play the role of an essential functional module. In binding studies of axonin-1 with NgCAM and NrCAM using domain deletion mutants, we found that the structural integrity and functional competence of axonin-1 required the presence all four domains (Rader et al., 1993; Fitzli et al., 2000). Therefore, we postulated that Igs 1–4 of axonin-1 form a conglomerate with a well-defined structure (Rader et al., 1996). In order to understand the role of axonin-1 in distinct cellular and developmental contexts at the atomic level we have analyzed axonin-$1_{Ig1–4}$ by

‡To whom correspondence should be addressed (e-mail: wolfram.welte@uni-konstanz.de).

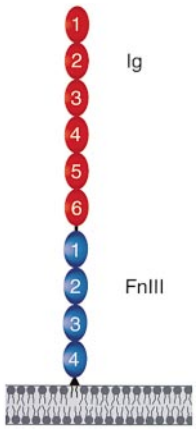

Figure 1. Domain Structure of the Neural Cell Adhesion Molecule Axonin-1/TAG-1

Axonin-1/TAG-1 is composed of six Ig domains that are arranged in a contiguous string in the N-terminal moiety. The C-terminal moiety of axonin-1/TAG-1 consists of four FnIII domains. A junctional decapeptide enriched in glycine and proline is interposed between the sixth Ig and the first FnIII domain. Axonin-1/TAG-1 is anchored to the cell membrane by a glycosylphosphatidylinositol group (for a detailed description: Furley et al., 1990; Zuellig et al., 1992). By domain deletion studies, the binding sites for the interactions of axonin-1 with NgCAM and NrCAM have been localized within the first four Ig domains (Rader et al., 1996; Fitzli et al., 2000). The results of binding studies with ligand CAMs and monoclonal antibodies further suggested that the first four Ig domains of axonin-1 form a unit that is structurally and functionally intact only when all for domains are present (Rader et al., 1996).

X-ray crystallography. We found that the four Ig domains are arranged in a U-shaped chain and form a compact molecule. In the crystals, the axonin-$1_{Ig1–4}$ molecules were aligned in a linear array. Adjacent axonin-$1_{Ig1–4}$ molecules were in an antiparallel orientation, their C termini pointing perpendicularly to the axis of the array. The intriguing arrangement of the axonin-$1_{Ig1–4}$ molecules in the crystal suggested a zipper mechanism as a molecular model for the cell–cell contact mediated by homophilic interactions of axonin-1 molecules. To test this model, two distinct mutations in a loop critical for the contact between axonin-$1_{Ig1–4}$ molecules were generated and expressed in myeloma cells. In confirmation of the suggested model, both mutations resulted in a complete loss of the homophilic binding capacity of axonin-1.

Results

The First Four Ig Domains of Axonin-1 Are Arranged in a U-Shaped Chain and Form a Compact Molecule

The structure of the first four Ig domains of axonin-1 has been solved at a resolution of 1.8 Å (for crystallographic data see Table 1). The overall structure of axonin-$1_{Ig1–4}$ is U-shaped due to contacts between domains 1 and 4 and domains 2 and 3 (Figure 2A). A linker of six residues connecting domains 2 and 3 provides sufficient interdomain flexibility to allow for the U-bend. This places the chain termini of the fragment only 15 Å apart from each other. Interactions between domains 1 and 4 and between domains 2 and 3 create a structure of roughly ellipsoid shape with a hole in its center (Figure 2A). The longest ellipsoid axis (95 Å) results from the length of two Ig domains in a tandem array, another axis (45 Å) results from the side-by-side packing of two domains, and the shortest axis (25 Å) corresponds roughly to the thickness of an Ig domain. The interactions between the Ig domains create a compact molecule. This is in accordance with previous predictions that were based on ligand and antibody binding studies with domain deletion mutants (Rader et al., 1996). Because the binding of NgCAM and the epitopes for several monoclonal antibodies were lost upon every single domain deletion among the first four Ig domains, a four-domain structure requiring the presence of all domains for structural integrity was postulated.

A similar U-shaped arrangement of four Ig domains was reported for the distantly related protein hemolin (26% identical residues), thought to be involved in a primitive form of immune response in insects (Su et al., 1998). Using a 3.8 Å cut-off, 190 out of 382 (or 49.5%) C_α atoms of axonin-$1_{Ig1–4}$ could be superimposed with those of hemolin at a root-mean-square deviation (rmsd) of 1.9 Å. The relatively low percentage of superimposed C_α positions results from a tilt of domains 1 and 4 of axonin-1 with respect to their hemolin counterparts by 5° and 15°, respectively. In addition, the buried surface between domains 1 and 4 is considerably smaller

Table 1. Data Collection and Phasing Statistics of a K_2PtCL_4 Derivatized and a Native Axonin-$1_{Ig1–4}$ Crystal

Data Set	Peak	Edge	Remote High	Remote Low	Native
Wavelength (Å)	1.0717	1.0720	0.9051	1.5418	0.9114
Resolution (Å)	15–2.8 (2.90–2.80)[a]	15–2.8 (2.90–2.80)	15–2.8 (2.90–2.80)	15–3.0 (3.11–3.00)	20–1.8 (1.86–1.80)
Unique reflections	12003	12019	12065	9600	48051
Completeness (%)	98.4 (96.8)	98.0 (92.9)	98.1 (95.0)	99.2 (97.3)	95.1 (83.3)
Average I/σ (I)	13.9 (2.5)	12.9 (2.3)	9.5 (2.0)	11.7 (2.7)	12.8 (3.6)
R_{sym}[b]	9.4 (43.1)	9.0 (39.2)	8.7 (35.3)	10.7 (39.4)	3.6 (20.6)
Phasing power[c] (acentrics)					
Dispersive	2.49	2.10	0	0.25	—
Anomalous	0.83	1.18	1.31	1.10	—
Figure of merit	—	—	0.47	—	—

[a] Values in parentheses correspond to the highest resolution shells.
[b] $R_{sym} = \Sigma_{hkl} \Sigma_i |I_{hkl} - <I_{hkl}>| / \Sigma_{hkl} \Sigma_i I_{hkl}$, where $<I_{hkl}>$ is the average of symmetry-related I_{hkl}.
[c] Phasing power is the mean value of heavy atom structure factor amplitude divided by lack of closure.

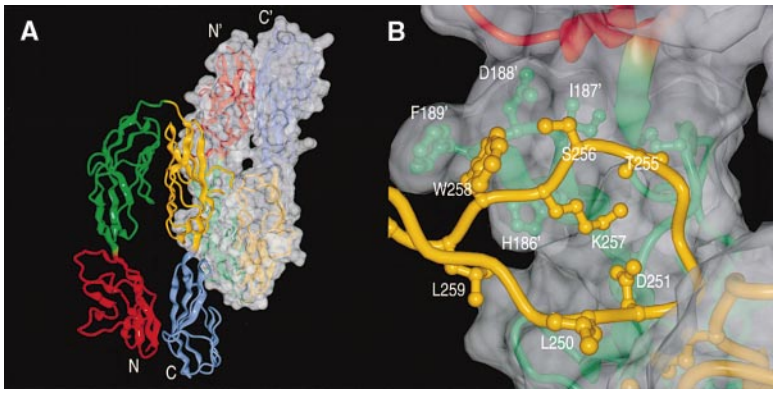

Figure 2. The Complex with the Largest Buried Surface of Two Crystallographically Equivalent Axonin-$1_{Ig1–4}$ Molecules

(A) Overview of the two axonin-$1_{Ig1–4}$ molecules shown in ribbon representation. Ig1–Ig4 are shown in red, green, yellow, and blue, respectively. One molecule is overlayed with its solvent-accessible surface. (B) Close-up view of the CE loop (shown in yellow) of Ig3 plugged into the central hole of the four Ig domains of the adjacent axonin-$1_{Ig1'–4'}$ molecule and approaching segments of Ig2′ and Ig3′ (shown in green and yellow, respectively). Some side chains of residues that contain atoms within 4 Å distance to atoms in the other molecule are shown and labeled. The important interactions are: a main chain hydrogen bond between S256 (Ig3) and D188′ (Ig2′); a hydrogen bond between a main chain oxygen of W258 (Ig3) and Nϵ of H186′ (Ig2′); a main chain hydrogen bond between W258 (Ig3) and D188′ (Ig2′); a hydrophobic interaction between W258 (Ig3) and F189′ (Ig2′). All figures were prepared with the program DINO (A. Philippsen, 2000, http://www.bioz.unibas.ch/∼xray/dino).

(910 Å^2) in axonin-$1_{Ig1–4}$ compared to hemolin (1220 Å^2), while the surface buried between domains 2 and 3 is similar in both (1259 Å^2 and 1382 Å^2, respectively).

In the Crystal, Axonin-$1_{Ig1–4}$ Molecules Are Arranged as a String with a Large Edge-to-Face Contact Surface and Antiparallel Orientation of Adjacent Molecules

In the crystal, the axonin-$1_{Ig1–4}$ molecules form two different contacts burying a surface of 750 Å^2 and 1260 Å^2 on each molecule, respectively, from contact with water. In the contact burying the larger surface, two of the U-shaped molecules arrange with antiparallel long axes so that the edge of one molecule contacts the face of the other (Figure 2A). As a central element of this interaction, one loop from Ig3 protrudes from the edge of an axonin-$1_{Ig1–4}$ molecule and contacts the central hole in the face of the adjacent molecule (Figure 2B). This loop formed by residues 250 to 261 connects strands in Ig3, which are labeled C and E according to the canonical Ig fold (Harpaz and Chotia, 1994). It contains 9 residues with atoms closer than 4 Å to the adjacent axonin-$1_{Ig1'–4'}$ molecule. Among these, three residues (250 to 252) interact with side chains from Ig3′, and seven residues (255 to 261) interact with the loop connecting strands F and G in Ig2′, mainly with residues 186 to 189 (Figure 2B). Interestingly, these strands and the connecting loop of Ig2 contain four additional residues compared to the corresponding segments of the other Ig domains (Figure 3). Therefore, the A′FGC sheet is longer in Ig2 than in the other Ig domains. Because in the crystals the CE loop of the Ig3 domain of one molecule interacts with this long FG loop in an adjacent molecule, we speculated that this contact is of critical importance for a specific interaction between axonin-1 molecules.

A role of this larger contact area between axonin-$1_{Ig1–4}$ molecules in biologically relevant interactions is further suggested by its unusually large surface. According to Janin (1997), the buried surface of serendipitous crystal contacts exhibits a mean area of 570 Å^2. Based on the results of this statistical study, the probability of finding a nonspecific interface of the size of the larger crystal contact between axonin-$1_{Ig1–4}$ molecules in a protein crystal is only 3.3%. Moreover, this contact is conserved among two further monoclinic crystal forms with different unit cell parameters and a triclinic crystal form (to be published elsewhere). It is worthwhile to note that the two sites for N-linked glycosylation found in axonin-$1_{Ig1–4}$ (Denzinger et al., 1997) are positioned such that the attached carbohydrate would not perturb the proposed contact.

Mutations in the FG Loop of the Second Ig Domain Result in the Loss of Homophilic Binding of Axonin-1

The hypothesis that a close interaction between the CE loop of Ig3 and the FG loop of Ig2′ of an adjacent axonin-1 molecule is a critical feature of the homophilic binding capacity of axonin-1 was tested by site-directed mutagenesis. Two variants of axonin-1 with mutations in the FG loop were designed, the double point mutant H186A/F189A and the deletion mutant DEL187–190. In the double point mutation H186A/F189A, the specific H bond interaction between the His186 side chain (FG loop of domain Ig2′) and the main chain carbonyl oxygen W258 (CE loop of Ig3) as well as the hydrophobic interaction of the F189 side chain (domain Ig2′) with a flat

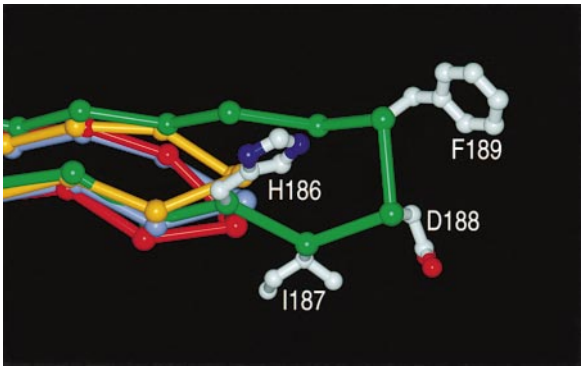

Figure 3. Comparison of the FG Loops in All Four Ig Domains

In the best overlay of all four domains, the C_α backbones of Ig1 (red), Ig3 (yellow), and Ig4 (blue) do not show marked differences. Ig2 (green) contains additional residues in strands F and G and the connecting loop. Of these, H186–F189 are interacting with the CE loop of Ig3 (Figure 2B).

hydrophobic depression of Ig3 are abolished. Because some of the strong hydrogen bonds established between the FG loop of Ig2′ and Ig3 of the adjacent axonin-$1_{Ig1–4}$ molecule are formed by main chain atoms, it appeared uncertain whether point mutations alone would result in a detectable reduction of the homophilic binding. We therefore constructed a second mutation, DEL187–190, in which the unusually long FG loop of Ig2 was converted into an "ordinary" FG loop, as found in Ig1, Ig3, and Ig4, by deleting the "extra" residues 187 to 190. To ensure that the reconstructed FG loop in Ig2 adopts a similar main chain conformation as in the other Ig domains, two point mutations were introduced at positions flanking the deletion. The K192G mutation was chosen, because a glycin occurs in the equivalent position of the other domains. The H186I mutation was introduced to stabilize the FG loop by a hydrophobic interaction of I186 with P136 of the BC loop, imitating a stabilizing interaction that is found between I285 and P241 of Ig3.

To assess the effect of the mutations on the homophilic binding function of axonin-1, the mutated forms were expressed in myeloma cells and their capacity of mediating cell–cell aggregation was compared with wild-type axonin-1. The mutated forms of axonin-1, DEL187–190 and H186A/F189A, were transfected into myeloma cells and stably expressing lines were selected. The obtained myeloma cell lines were termed M-DEL187–190 and M-H186A/F189A, respectively. By subcloning, cell lines were isolated that exhibited expression levels of the mutant axonin-1 proteins comparable to a reference cell line, M-axonin-1 (Rader et al., 1993), expressing wild-type axonin-1 (Figure 4A). The heterotopicly expressed axonin-1 was present on the surface of the myeloma cells, as evidenced by indirect immunofluorescence (Figure 4B, right column), indicating that the proteins are correctly transported to the cell surface.

As shown in Figure 4B (left columns), both mutations of axonin-1 resulted in a complete loss of the homophilic binding capacity, whereas myeloma cells of line M-axonin-1, which express wild-type axonin-1, aggregate to large clumps of cells due to homophilic binding of their surface-exposed axonin-1 molecules (for a detailed analysis see Rader et al., 1993). These results strongly support the role of the intermolecular interaction between the CE loop of Ig3 and the FG loop of Ig2 for axonin-1-mediated homophilic cell adhesion.

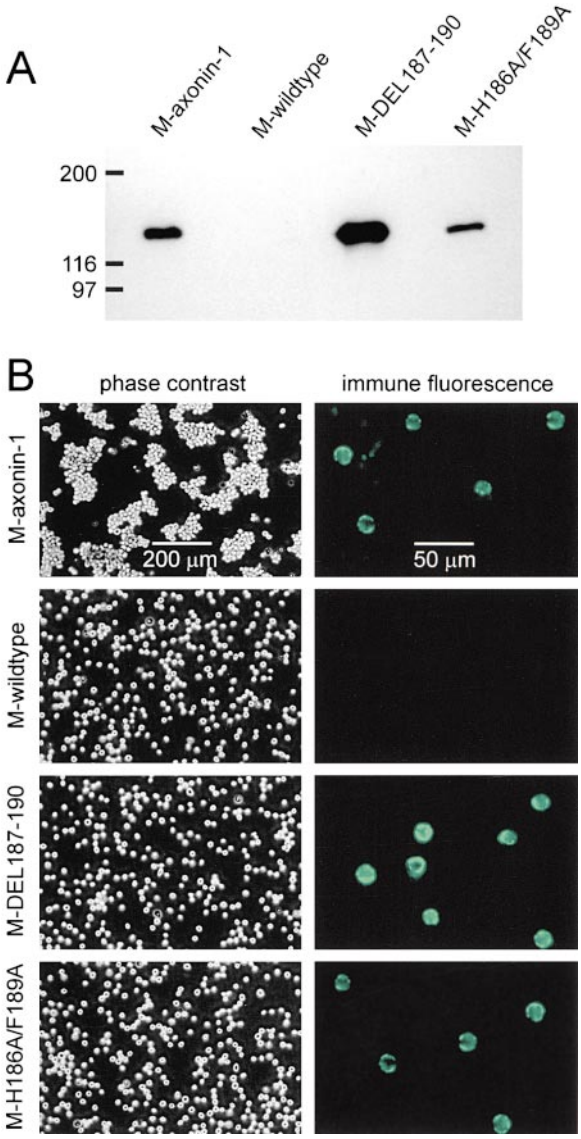

Figure 4. Loss of Homophilic Binding by Mutations in the FG Loop of the Second Ig Domain of Axonin-1

The role of the close interaction between the CE loop of Ig3 and the FG loop of Ig2 of an adjacent axonin-1 molecule for the homphilic *trans*-interaction of axonin-1 was investigated by site-directed mutagenesis. Two variants of axonin-1 with mutations within the FG loop of Ig2, DEL187–190 and H186A/F189A, respectively, were generated and expressed in myeloma cells. The effect of the mutations on homophilic *trans* binding of axonin-1 was studied in cell aggregation assays, by comparing with myeloma cells expressing wild-type axonin-1.

(A) Western blot analysis of wild-type and mutated axonin-1 heterologously expressed in myeloma cells. M-axonin-1, myeloma cell line expressing wild-type axonin-1. M-wildtype, nontransfected myeloma cells. M-DEL187–190, myeloma cell line expressing the DEL187–190 mutation of axonin-1. M-H186A/F189A, myeloma cell line expressing the H186A/F189A double point mutation of axonin-1.

(B) Phase contrast images (left column) and immunofluorescence images (right column) of myeloma cells. A pronounced aggregation was found with the myeloma cells expressing wild-type axonin-1 (M-axonin-1). In contrast, myeloma cells expressing the mutated forms of axonin-1 and nontransfected myeloma cells did not form aggregates.

Discussion

The Homophilic Interaction between Axonin-$1_{Ig1–4}$ Molecules May Involve an Induced Fit Mechanism

Immunoglobulin domains are commonly classified into V, C1, C2, and I sets (Harpaz and Chotia, 1994). The first four domains of axonin-1 have been predicted to belong to the I set, whose members consist of two β sheets formed by strands ABED and strands A′FGCC′ (Figure 5). Analogous to the discrimination between the C1 and C2 set, a subdivision of the I set into I1 and I2 has been suggested, depending on whether or not a D strand

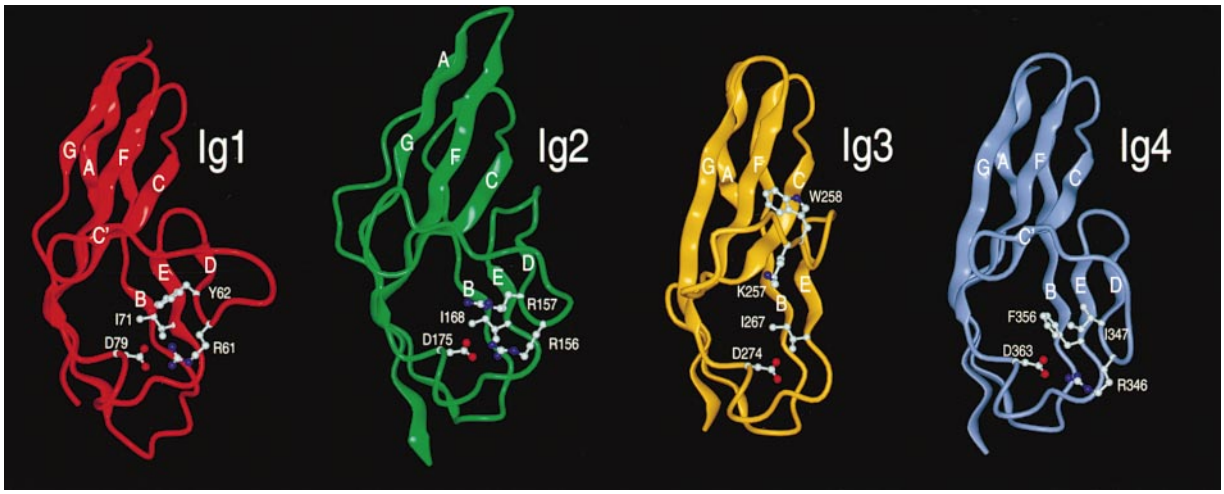

Figure 5. Indications for an Induced Fit

Ig1–Ig4 are shown in ribbon representation from left to right. Ig1, Ig2, and Ig4 show the typical way that strand D is stabilized in I1 set topology by fixation of the loop before strand D to the loop following strand E. The four key residues for the stabilization are shown: In Ig4, R346 and I347 from the former are forming a salt bridge and a hydrophobic patch with D263 and F356 from the latter. In Ig3 strand D is nonexistent although residues capable of forming equivalent interactions are found at equivalent positions in the sequence and those from the loop following strand E are at the same positions as in Ig4 (K257, W258, D274, and I267, respectively).

is present (Casanovas et al., 1998). According to this classification, Ig1 and Ig4 exhibit ideal set I1 topology, while Ig2 lacks the short C′ strand, a fact that has also been reported for other members of the I1 subset. Ig3 cannot easily be classified as it lacks both strands C′ and D. Apart from the structure between strands C and E, it most closely resembles Ig4 of both axonin-1 and hemolin, and the Ig-like domain of telokin (Holden et al., 1992), all clear set I1 members. We therefore propose to classify Ig3 as a member of the I1 set that lacks strand D, rather than to classify it as a member of I2.

In a standard I1 set architecture, strand D starts with a basic residue that forms a salt bridge with a conserved aspartate from the EF loop. This residue is followed by a hydrophobic residue that interacts mainly with a hydrophobic residue from strand E, as seen in Ig1, Ig2, and Ig4 (Figure 5). In Ig3 of axonin-1, the basic and the subsequent hydrophobic residue of strand D are represented by K257 and W258, respectively. They are at the expected positions in the sequence and, therefore, could contribute to the formation of a strand D. Furthermore, in the EF loop their putative partners, a glutamate and an isoleucine, are suitably positioned for the expected I1 set interaction (Figure 5). However, in the structure of Ig3 that is observed in the crystal, strand D is missing. Moreover, W258 of Ig3, rather than interacting with a hydrophobic residue of strand E within Ig3, interacts with Ig2′ of the adjacent molecule by contacting F189′ from the FG loop and by forming two intermolecular hydrogen bonds with its main chain atoms. This discrepancy between the expected and the observed structure together with the involvement of W258 in an intermolecular interaction suggests an induced fit rearrangement of residues between strands C and E upon complex formation. In combination, the large buried surface and the evidence for an induced fit mechanism suggests a rather high affinity for the antiparallel association of axonin-$1_{Ig1–4}$.

Axonin-1-Mediated Cell–Cell Adhesion Involves a Zipper-like String of Axonin-1 Molecules from Apposed Membranes

In the crystal, each single axonin-$1_{Ig1–4}$ simultaneously acts both as a “donor” and as an “acceptor” of a CE loop. Consequently, the edge-to-face packed axonin-$1_{Ig1–4}$ molecules form a linear string with the C termini of adjacent molecules oriented perpendicular to the string and antiparallel to each other (Figure 6). Indeed, the crystallographic 2-fold screw axis transforms the set of molecules with the C termini pointing in the same direction into the set of interposed molecules having their C termini oriented oppositely. This suggests that axonin-1 molecules engaged in a homophilic *trans*-interaction are alternately provided from the two apposed cell surfaces and form a zipper-like linear string (Figure 7). It has been sugested that a zipper mechanism may represent an efficient way to form and expand a stable cell–cell contact (for a discussion see Shapiro et al., 1995, but see also Pertz et al., 1999). Compared with a pairwise capping mechanisms (Singer, 1992), a zipper may be advantageous. Zippers grow or shrink mostly at their ends but are stable in between. If axonin-1 molecules are present in both membranes outside of a zipper, and if the distance of the membranes allows for the *trans*-interaction, they will be recruited by the zipper because of its favorable energy of formation. The high mobility of GPI-anchored proteins in the membrane may contribute to a high growth rate (Van der Merwe and Barclay, 1994). Indeed, in an immunoelectron microscopic study of growth cones growing on an axonin-1 substratum, all axonin-1 accumulated in the contact

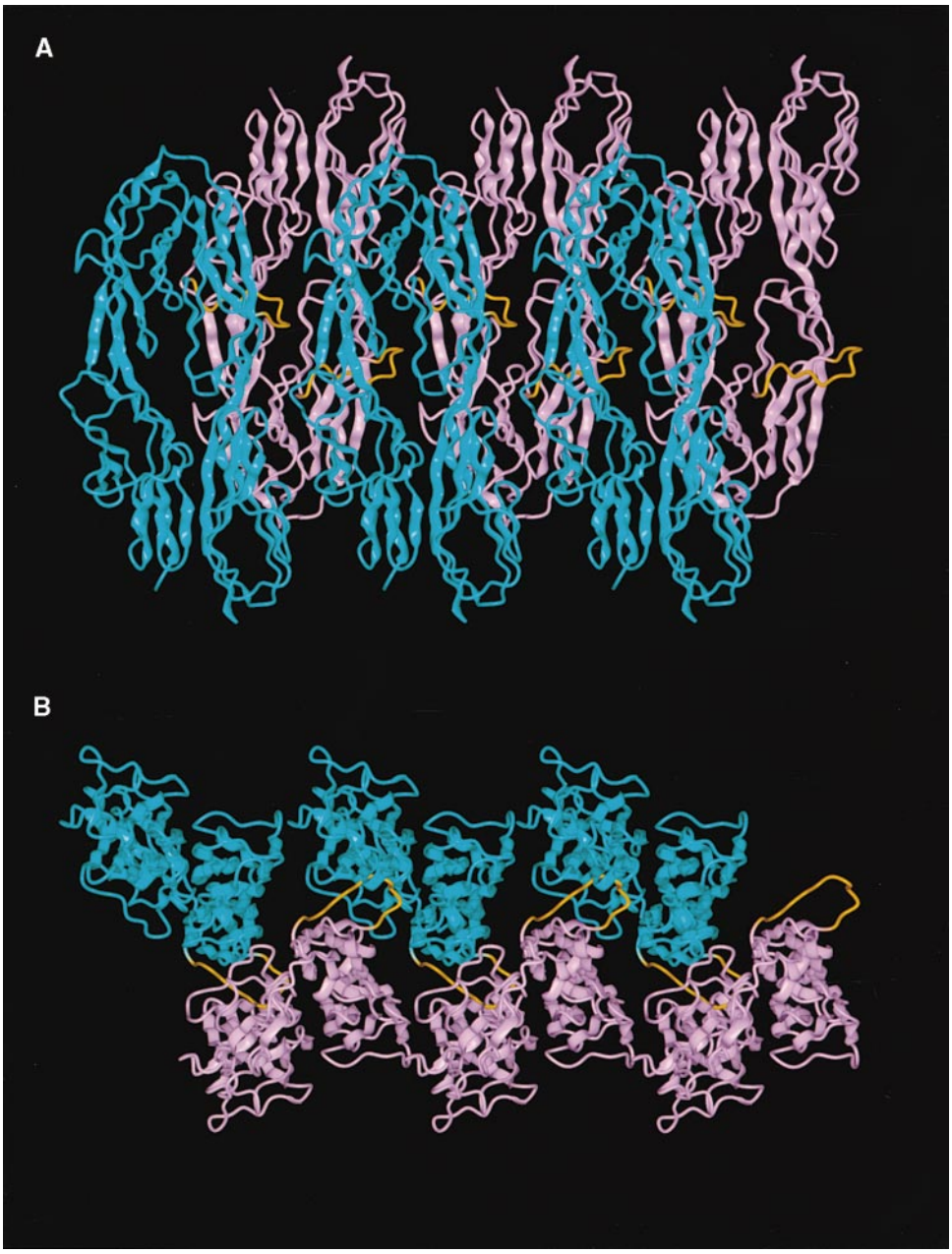

Figure 6. View of the String of Axonin-$1_{Ig1–4}$ Molecules in the Crystal

(A) View perpendicular to the long axes of the molecules and the 2-fold crystallographic screw axis that relates the molecules shown in cyan to those shown in magenta; (B) View along the long axes of the molecules after rotation by 90° around the 2-fold crystallographic screw axis.

area and a complete depletion of axonin-1 outside of the contact area was observed (Stoeckli et al., 1996).

A Homophilic *cis* Binding Site in the FnIII Region May Mediate a Side-by-Side Alignment of Linear Strings of *trans*-Bound Axonin-1

Many cell–cell contacts assume a two-dimensional apposition of the membranes. In some situations, multiple zipper-like strings in random orientation may provide sufficient adhesive force to maintain such a contact. To generate a higher adhesive force, it may be necessary to increase the density of *trans*-bound molecules by a parallel alignment of the linear strings. From the contacts among the axonin-$1_{Ig1–4}$ molecules in the crystals, no additional obvious interactions, which would allow for a parallel association of the strings, are suggested. However, a recent observation of a homophilic interaction between the FnIII repeats of TAX-1, the human homolog of axonin-1 (Tsiotra et al., 1996), may provide a clue on how axonin-1 molecules may interact to form a side-by-side arrangement of strings. Using TAX-1 truncated after the FnIII domains, Tsiotra and colleagues found a

strong homophilic adhesion mediated by FnIII moieties. Because the FnIII moieties are located close to the membrane, a *cis*-interaction between FnIII moieties of axonin-1 molecules in the plane of the same membrane (*cis*-interaction) is more likely than an interaction with molecules from an apposed membrane. By *cis*-interactions between FnIII domains of axonin-1 molecules, linear axonin-1 strings could be linked laterally to form two-dimensional arrays that establish a contact area.

The highest density of axonin-1 molecules involved in homophilic *trans*-interaction, and thereby the highest adhesive strength per molecule in a contact area is obtained when all axonin-1 molecules are engaged in a zipper array. Because the local surface concentrations of axonin-1 in two contacting cells will never match perfectly due to different expression levels or concentration fluctuations, some fraction of axonin-1 will not be recruited in a zipper array. As unbound axonin-1 cannot become integrated into the interior of the zipper, it should not form *cis*-links with the zipper array and be excluded from it. Therefore, the homophilic *cis* binding site in the FnIII part should not be available in monomeric, unbound axonin-1. The conformation of axonin-1 in the monomeric state, as seen in negative-staining EM, suggests that this may indeed be the case. Monomeric axonin-1 was found to assume a backfolded "horseshoe" conformation (Figure 7) with the N terminus located close to the C terminus near the membrane (Rader et al., 1996). Based on observations made with domain deletion mutants of axonin-1, the backfolded structure is stabilized by an intramolecular interaction involving the fourth FnIII domain (Rader et al., 1996). The exclusive occurrence of the backfolded axonin-1 in electron micrographs indicates a strong interaction of the involved domains. It is, therefore, conceivable that in the backfolded conformation the homophilic site in the FnIII moiety is masked. In accordance with this assumption, axonin-1 molecules on the surface of single cells (that are not engaged in a cell–cell contact) remain randomly distributed (Buchstaller et al., 1996). Based on steric consideration, the association of monomeric axonin-1 with an axonin-1 zipper involves most likely a transition from the backfolded into an extended form. In the extended structure, the homophilic binding site on the FnIII moiety is accessible and *cis* bindings with other axonin-1 molecules involved in zipper arrays may be established. Monomeric axonin-1 molecules would remain mobile and eventually be "squeezed" out of the zipper array. This would further the chance of monomeric axonin-1 molecules to become correctly integrated into a string at one of its ends, thereby enhancing the expansion of the two-dimensional zipper array at cell–cell contact areas. Our model also predicts an enrichment of GPI anchors in the apposed membranes.

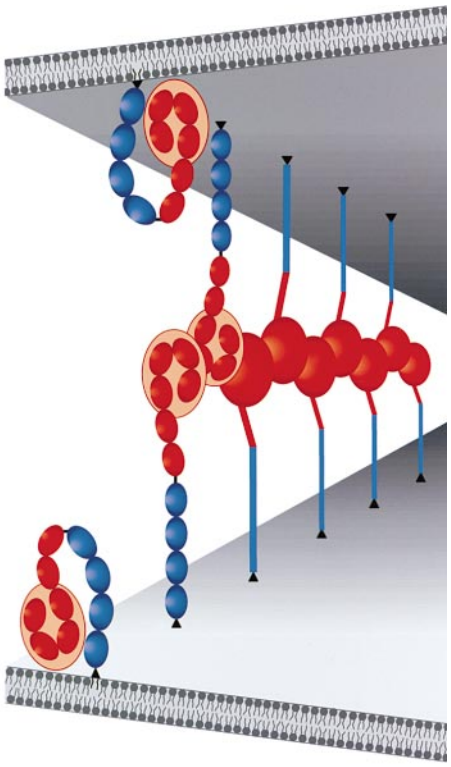

Figure 7. A Model for Cell–Cell Adhesion Mediated by a Zipper-like Linear Array of Axonin-1 Molecules Originating Alternately from the Apposed Membranes

The crystal structure suggests a zipper model as the basis for the homophilic interaction of axonin-1 molecules involved in an adhesive contact between the membranes of apposed cells. While monomeric axonin-1 molecules are preferably in a backfolded, "horseshoe"-like conformation (Rader et al., 1996), axonin-1 molecules engaged in a homophilic *cis*-interaction are assumed to be in the extended conformation. It is possible that in the backfolded "horseshoe" conformation, the homophilic binding site in the FnIII moiety is masked. This would ensure that the homophilic site in the FnIII region is selectively active in crosslinking axonin-1 molecules involved in a zipper.

Concluding Remarks

The generation of a compact four-domain module may be a structural feature found also in other IgSF-CAMs. Binding studies with NgCAM (Kunz et al., 1998), the homolg of human L1, and NrCAM (Fitzli et al., 2000) revealed a complete loss of homophilic binding after deletion of each one of the first four Ig domains. As in axonin-1, these results may reflect the importance of each one of the domains for the structural integrity of the Ig 1–4 module rather than the participation of all four domains in direct ligand contact. Because the first four Ig domains of axonin-1, as well as those of NgCAM and NrCAM, are not only involved in homphilic interactions, but also in the respective heterophilic contacts, it is tempting to speculate that the formation of a four-domain module in these IgSF-CAMs provides the molecular scaffold on which the capacity of engaging in multiple interactions has evolved in this family of versatile molecules.

Experimental Procedures

Protein Expression, Refolding, and Purification

The cDNA encoding amino acids 1–403 of chicken axonin-1 was cloned into the T7 expression vector pTFT and expressed in *Escherichia coli* BL21-DE3. The resulting protein contained six additional histidine residues and a factor Xa cleavage site at the N terminus.

The protein was recovered from inclusion bodies by 8 M urea. Axonin-$1_{Ig1–4}$ was purified under denaturing conditions using Nickel-NTA-Sepharose (Qiagen) and refolded according to standard procedures (Buchner and Rudolph, 1991). Aggregated protein was removed by gel filtration on Sephacryl S200 (Pharmacia). MALDI mass spectrometry showed that the N-terminal His tag was cleaved off during the refolding process.

Crystallization

Crystals were grown at 17°C using the sitting-drop vapor diffusion method. Equal volumes of reservoir and protein solution (at a concentration of 8 mg/ml in 25 mM Tris-HCl, 125 mM NaCl, pH 8.5) were mixed. The reservoir solution contained 15%–17% w/v PEG 10000, 150 mM sodium formiate, and 100 mM HEPES, pH 7.5. For derivatization crystals were soaked in 0.5 mM K_2PtCl_4 in reservoir solution for 10 hr. Crystals belonged to space group $P2_1$ with one molecule in the asymmetric unit and cell dimensions of a = 60.3 Å, b = 43.4 Å, c = 94.0 Å, and β = 96.7° for the native and a = 60.6 Å, b = 45.5 Å, c = 99.6 Å, and β = 96.1° for the platinum derivatized crystal. They were flash frozen by plunging into liquid nitrogen using 20% v/v glycerol as a cryoprotectant and maintained at 100 K in a nitrogen cold stream during data collection. Data were processed with DENZO/SCALEPACK (Otwinowski and Minor, 1997) and with XDS (Kabsch, 1988).

Structure Determination and Refinement

The structure was determined using MAD data, collected from the platinum derivatized crystal at four wavelengths (1.0720 Å, 1.0717 Å and 0.9051 Å at beamline X31 at EMBL/DESY, Hamburg, and 1.5418 Å at a rotating anode generator). Data collection and phasing statistics are listed in Table 1. The platinum sites were found with SOLVE (Terwilliger and Berendzen, 1999). A refinement of the heavy-atom parameters and the calculation of the phases were carried out using SHARP (De la Fortelle and Bricogone, 1997). SOLOMON (Abrahams and Leslie, 1996) was used for solvent flattening. Map interpretation and model building were carried out using the program O (Jones et al., 1991). The model was refined against a native, high-resolution data set obtained at beamline X11 at EMBL/DESY, Hamburg. CNS (Brünger et al., 1998) (Version 0.4) was used to carry out the refinement. Energy minimization, simulated annealing, and individual temperature factor refinement were used, alternated by manual model rebuilding. A solvent mask correction and an overall anisotropic temperature factor were applied. The final model contains amino acids 7–388, 357 water molecules and 1 glyerol. Using all reflections > 0 in the resolution range 20–1.8 Å, the R_{cryst} is 22.6% and the R_{free} for 5% of all reflections is 25.7%. Residues D188 and N145 have disallowed main chain torsion angles in the Ramachandran plot. D188 plays a key role in protein–protein interactions, and N145 is located in a sharp turn directly after strand C of Ig2. For both residues clear electron density is present.

Construction of Mutant Expression Vectors

Expression of axonin-1 in myeloma cell line J558L is based on expression vector pMAX (16.6 kb) described by Rader et al. (1993). An 1102 bp fragment covering the N-terminal part of the axonin-1 sequence including the site to be mutated was subcloned into pBluescript KS^- using the unique restriction sites EcoRI and BamHI present within the axonin-1 sequence. Mutagenesis was carried out using the "quick change method" following the protocol provided by STRATAGENE. The sequences of the mutagenic oligonucleotide primers are given below, the site of mutation depicted in italics. Oligo H186A/F189A forward: 5′-GC TTT GCC ACC AGC *GC*C ATC GAC *GC*C ATC ACC AAG AGC G-3′. Oligo H186A/F189A backward: 3′-CG AAA CGG TGG TCG *CG*G TAG CTG *CG*G TAG TGG TTC TCG C-5′. Oligo DEL187–190 forward: 5′-CG TGC TTT GCC ACC AGC *ATC* ACC *GGG* AGC GTT TTC AGC AAG-3′. Oligo DEL187–190 backward: 3′-GC ACG AAA CGG TGG TCG *TA*G TGG *CC*C TCG CAA AAG TCG TTC-5′.

The presence of the desired mutations in the resulting pBluescript KS^- constructs was confirmed by DNA sequencing and the EcoRI/BamHI fragments of successfully mutated pBluescript KS^- constructs were recloned into the expression vector pMAX. Resulting mutated pMAX constructs were analyzed again by DNA sequencing to rule out any contamination by wild-type pMAX vector and to confirm the identity of the mutations in the final expression constructs.

Protoblast Fusion and Cell Cultivation

Transfection of wild-type myeloma cells J558L with expression constructs pMAX-H186A/F189A and pMAX-DEL187–190 by protoblast fusion was carried out as described by Oi et al. (1983). After two days of incubation, transfected cells were selected by addition of 5 mM L-histidinol (Sigma). Independent transfectants were selected by limiting dilution of the cells in DMEM (GIBCO/Life Technologies) containing 10% FCS, 1 mM sodium pyruvate, 2 mM glutamine, 0.05 mM β-mercaptoethanol in 96-well plates (Nunc) at 37°C with 10% CO_2.

Western Blot/Axonin-1 Immunodetection

Samples of cell lysates for SDS-PAGE were prepared from cultures at cell densities of 0.5–1.0 $\times$ 10^6 cells/ml. After centrifugation, cells were resuspended in PBS (150 mM sodium chloride, 25 mM sodium phosphate, pH 7.5) and mixed with SDS-PAGE sample buffer, at a density of 10_4 cells/μl. SDS-PAGE and transfer to a nitrocellulose membrane was carried out following standard protocols. An equivalent of 5 $\times$ 10_4 cells were loaded per lane. Axonin-1 immunodetection: after blocking (1% blocking reagent [Boehringer Mannheim], 150 mM NaCl, 0.05% Tween-20 in 25 mM Tris/HCl pH 7.5 [TBST]), membranes were incubated in a polyclonal rabbit anti-axonin-1 serum (1/5000 in TBST) followed by peroxidase-conjugated goat anti-rabbit IgG (Bioscience) (1/5000 in TBST, 1 hr). Axonin-1 bands were visualized by chemoluminescence using reagents from Boehringer Mannheim. All steps were carried out at room temperature.

Immunofluorescence Staining of Myeloma Cells

For immunofluorescence, cells were washed with 1% FCS in PBS and incubated with a rabbit anti-axonin-1 serum diluted 1/500 in 1% FCS/PBS for 1 hr followed by FITC-labeled goat anti-rabbit IgG (Cappel) (1/100 in 1% FCS/PBS for 1 hr). After washing twice with 1% FCS/PBS, cells were fixed in 4% paraformaldehyde in PBS for 10 min, washed twice with PBS and mounted.

Acknowledgments

We gratefully acknowledge help by Simone Müller, Joachim Diez, and Ana Gonzalez and thank Claudia Stürmer for useful discussions and Esther Stoeckli for critical reading of the manuscript. The graphical artwork of Figures 1 and 7 was performed by Iwon Blum. The work was supported by grants from the Swiss National Science Foundation and the EC Biotechnology program 2 (P. S.) and the Deutsche Forschungsgemeinschaft (W. W.).

Received September 17, 1999; revised April 20, 2000.

References

Abrahams, J.P., and Leslie, G.W. (1996). Methods used in the structural determination of bovine mitochondrial F1 ATPase. Acta Crystallogr. *D52*, 30–42.

Brümmendorf, T., and Rathjen, F.G. (1996). Structure/function relationships of axon-associated adhesion receptors of the immunoglobulin superfamily. Curr. Opin. Neurobiol. *6*, 584–593.

Brünger, A.T., Adams, P.D., Clore, G.M., DeLano, W.L., Gros, P., Grosse-Kunstleve, R.W., Jiang, J.-S., Kuszewski, J., Nilges, M., Pannu, N.S., Read, R.J., Rice, L.M., Simonson, T., and Warren, G.L. (1998). Crystallography and NMR system: a new software suite for macromolecular structure determination. Acta Crystallogr. *D54*, 905–921.

Buchner, J., and Rudolph, R. (1991). Renaturation, purification and characterization of recombinant Fab-fragments produced in *Escherichia coli*. Biotechnology *9*, 157–162.

Buchstaller, A., Kunz, S., Berger, P., Rader, C., Ziegler, U., and Sonderegger, P. (1996). The cell adhesion molecules NgCAM and axonin-1 form heterodimers in the neuronal membrane and cooperate in neurite outgrowth promotion. J. Cell Biol. *135*, 1593–1607.

Burgoon, M.P., Grumet, M., Mauro, V., Edelman, G.M., and Cunningham, B.A. (1991). Structure of the chicken neuron-glia cell adhesion molecule, NgCAM: origin of the polypeptides and relation to the Ig superfamily. J. Cell Biol. *130*, 733–744.

Casanovas, J.M., Stehle, T., Liu, J.-H., Wang, J.-H., and Springer, T.A. (1998). A dimeric crystal structure for the N-terminal two domains of intercellular adhesion molecule-1. Proc. Natl. Acad. Sci. USA *95*, 4134–4139.

Chothia, C., and Jones, Y.E. (1997). The molecular structure of cell adhesion molecules. Annu. Rev. Biochem. *66*, 823–862.

De la Fortelle, E., and Bricogone, G. (1997). SHARP: a maximum likelihood heavy-atom parameter refinement program for the MIR and MAD methods. Methods Enzymol. *276*, 472–494.

Denzinger, T., Przybylski, M., Savoca, R., and Sonderegger, P. (1997). Mass spectrometric characterisation of primary structure, sequence heterogeneity and intramolecular disulfide loops of the cell adhesion protein axonin-1 from chicken. Eur. Mass Spect. *3*, 379–389.

Felsenfeld, D.P., Hynes, M.A., Skoler, K.M., Furley, A.J., and Jessell, T.M. (1994). TAG-1 can mediate homophilic binding, but neurite outgrowth on TAG-1 requires an L1-like molecule and β1 integrins. Neuron *12*, 675–690.

Fitzli, D., Stoeckli, E.T., Kunz, S., Siribour, K., Rader, C., Kunz, B., Kozlov, S.V., Buchstaller, A., Lane, R.P., Suter, D.M., et al. (2000). A direct interaction of axonin-1 with NrCAM results in guidance, but not growth of commissural axons. J. Cell Biol., in press.

Furley, A.J., Mortun, S.B., Manalo, D., Karagogeos, D., Dodd, J., and Jessell, T.M. (1990). The axonal glycoprotein TAG-1 is an immunoglobulin superfamily member with neurite outgrowth promoting activity. Cell *61*, 157–170.

Harpaz, Y., and Chotia, C. (1994). Many of the immunoglobulin superfamily domains in cell adhesion molecules and surface receptors belong to a new structural set which is close to that containing variable domains. J. Mol. Biol. *238*, 528–539.

Holden, H.M., Ito, M., Hartshorne, D.J., and Rayment, I. (1992). X-ray structure determination of telokin, the C-terminal domain of myosin light chain kinase, at 2.8 Å resolution. J. Mol. Biol. *227*, 840–851.

Janin, J. (1997). Specific versus non-specific contacts in protein crystals. Nature Struct. Biol. *4*, 973–974.

Jones, T.A., Zou, J.Y., Cowan, S.W., and Kjeldgaard, M. (1991). Improved methods for building protein models in electron density maps and the loction of errors in these models. Acta Crystallogr. *A47*, 110–119.

Kabsch, W. (1988). Evaluation of single crystal X-ray diffraction from a position sensitive detector. J. Appl. Crystallogr. *21*, 916–924.

Kunz, S., Ziegler, U., Kunz, B., and Sonderegger, P. (1996). Intracellular signaling is changed after clustering of the neural cell adhesion molecules axonin-1 and NgCAM during neurite fasciculation. J. Cell Biol. *135*, 253–267.

Kunz, S., Spirig, M., Ginsburg, C., Buchstaller, A., Berger, P., Lanz, R., Rader, C., Vogt, L., Kunz, B., and Sonderegger, P. (1998). Neurite fasciculation mediated by complexes of axonin-1 and Ng CAM. J. Cell Biol. *143*, 1673–1690.

Lustig, M., Sakurai, T., and Grumet, M. (1999). Nr-CAM promotes neurite outgrowth from peripheral ganglia by a mechanism involving axonin-1 as a neuronal receptor. Development *209*, 340–351.

Moos, M., Tacke, R., Scherer, H., Teplow, D., Früh, K., and Schachner, M. (1988). Neural adhesion molecule L1 as a member of the immunoglobulin superfamily with binding domains similar to fibronectin. Nature *334*, 701–703.

Oi, V.T., Morrison, S.L., Herzenberg, L.A., and Berg, P. (1983). Immunoglobuline gene expression in transformed lymphoid cells. Proc. Natl. Acad. Sci. USA *80*, 825–829.

Otwinowski, Z., and Minor, W. (1997). Processing of X-ray diffraction data collected in oscillation mode. Methods Enzymol. *276*, 307–326.

Pertz, O., Bozic, D., Koch, A.W., Fauser, C., Brancaccio, A., and Engel, J. (1999). A new crystal structure, Ca^{2+} dependence and mutational analysis reveal molecular details of E-cadherin homoassociation. EMBO J. *18*, 1738–1747.

Rader, C., Stoeckli, E.T., Ziegler, U., Osterwalder, T., Kunz, B., and Sonderegger, P. (1993). Cell–cell adhesion by homophilic interaction of the neural cell recognition molecule axonin-1. Eur. J. Biochem. *215*, 133–141.

Rader, C., Kunz, B., Lierheimer, R., Giger, R.J., Berger, P., Tittmann, P., Gross, H., and Sonderegger, P. (1996). Implications for the domain arrangement of axonin-1 derived from the mapping of its NgCAM binding site. EMBO J. *15*, 2056–2068.

Rathjen, F.G., Wolff, J.M., Frank, R., Bonhoeffer, F., and Rutishauser, U. (1987). Membrane glycoproteins involved in neurite fasciculation. J. Cell Biol. *104*, 343–353.

Shapiro, L., Fannon, A.M., Kwong, P.D., Thompson, A., Lehmann, M.S., Grübel, G., Legrand, J.F., Als-Nielsen, J., Colman, D.R., and Hendrickson, W.A. (1995). Structural basis of cell–cell adhesion by cadherins. Nature *374*, 327–337.

Singer, S.J. (1992). Intercellular communication and cell–cell adhesion. Science *255*, 1671–1677.

Stoeckli, E.T., and Landmesser, L.T. (1995). Axonin-1, NrCAM and NgCAM play different roles in the in vivo guidance of chick commissural neurons. Neuron *14*, 1165–1179.

Stoeckli, E.T., Ziegler, U., Bleiker, A., Groscurth, P., and Sonderegger, P. (1996). Clustering and functional cooperation of NgCAM and axonin-1 in the substratum-contact area of growth cones. Dev. Biol. *177*, 15–29.

Su, X.-D., Gastinel, L.N., Vaughn, D.E., Faye, I., Poon, P., and Bjorkmann, P.J. (1998). Crystal structure of hemolin: a horseshoe shape with implications for homophilic adhesion. Science *281*, 991–995.

Terwilliger, T.C., and Berendzen, J. (1999). Automated structure solution for MIR and MAD. Acta Crystallogr. *D55*, 849–861.

Tessier-Lavigne, M., and Goodman, C.S. (1996). The molecular biology of axon guidance. Science *274*, 1123–1133.

Tsiotra, P.C., Theodorakis, K., Papamatheakis, J., and Karagogeos, D. (1996). The fibronectin domains of the neural adhesion molecule TAX-1 are necessary and sufficient for homophilic binding. J. Biol. Chem. *46*, 29216–29222.

Van der Merwe, P.A., and Barclay, A.N. (1994). Transient intercellular adhesion: the importance of weak protein–protein interactions. Trends Biol. Sci. *19*, 354–358.

Zuellig, R.A., Rader, C., Schroeder, A., Kalousek, M.B., von Bohlen und Halbach, F., Osterwalder, T., Inan, C., Stoeckli, E.T., Affolter, H.U., Fritz, A., et al. (1992). The axonally secreted cell adhesion molecule, axonin-1: primary structure, immunoglobulin- and fibronectin type-III-like domains, and glycosylphosphatidylinositol anchorage. Eur. J. Biochem. *204*, 453–464.

Protein Data Bank ID Code

The coordinates were deposited at the Protein Data Bank under ID code 1CS6.